HYDROLOGICAL PROCESSES
Hydrol. Process. **16**, 1301–1317 (2002)
Published online in Wiley InterScience (www.interscience.wiley.com). DOI: 10.1002/hyp.1063

Impact of soil surface moisture initialization on rainfall in a limited area model: a case study of the 1995 South Ticino flash flood

C. Cassardo,[1]* G. P. Balsamo,[1,2] C. Cacciamani,[3] D. Cesari,[3] T. Paccagnella[3] and R. Pelosini[2]

[1] *Department of General Physics, University of Turin, Turin, Italy*
[2] *Regional Meteorological Service, Piedmont Region, Turin, Italy*
[3] *Regional Meteorological Service (ARPA–SMR), Bologna, Italy*

Abstract:

The influence of the soil moisture initialization on predicting rainfall in a limited-area model (LAM) was analysed. The model selected for the simulation was the LAM of Bologna (LAMBO). The case study selected in this paper was the flash flood episode that occurred during September 1995 in the South Ticino area (Switzerland). Two different experiments were conducted. In the first experiment, all initial fields including the initial soil moisture were provided by European Centre for Medium-range Weather Forecast (ECMWF) analyses. In the second one, the initial soil moisture fields were calculated by running a soil–vegetation–atmosphere transfer scheme (the Land Surface Process Model—LSPM) in stand-alone mode. The LSPM was driven by the synoptic observations carried out on a mesoscale area that includes Northern Italy. In order to overcome the well-known problem of the initial soil moisture content, LSPM was run for a long period (5 months) preceding the flood, in order to reach a stability state. The soil moisture field calculated by LSPM is more structured than the ECMWF one, and the numerical values of soil moisture are generally lower than those of ECMWF. The results seemed to indicate that the precipitation field obtained for the flood episode in the second experiment is closer to the observations than in the control run, even if there were still some underestimations. The precipitation peak modelled on South Ticino was closer to the observations, and this result seems to confirm the importance of the correct initialization of the soil moisture field even in cases of short-range forecasting. Copyright © 2002 John Wiley & Sons, Ltd.

KEY WORDS flood; soil moisture; initialization; limited-area model (LAM); Mesoscale Alpine Programme (MAP); Land Surface Process Model (LSPM); prediction; LAM Bologna (LAMBO); climatology of parameters at the surface (CLIPS) experiment

INTRODUCTION

The important feedback processes between soil and atmosphere, particularly concerning the water vapour cycle, are commonly known. The influence of the soil wetness on the climatic system has been analysed both using observations and model predictions by many authors since 1980 (Shukla and Mintz, 1982; Rowntree and Bolton, 1983; Betts and Ball, 1995; Burde *et al.*, 1996; Zeng *et al.*, 1996; Schär *et al.*, 1996; Eltahir, 1998). The seasonal water storage in the soil can introduce longer-term memory effects with a time scale of several months, and the importance of a realistic initialization of soil moisture in numerical models for climatic simulations is recognized as a key factor in their performance (Mahfouf, 1991; Viterbo, 1995; Beljaars *et al.*, 1996). Less well known and less analysed is the importance of the soil moisture initialization for short-term numerical predictions, even if the evidence of some recent observations (Findell and Eltahir, 1997) and

* Correspondence to: C. Cassardo, Department of General Physics "A Avogadro", University of Tonno, Via Pietro Giuna 1-1-10125, Tonno, Italy. E-mail: cassardo@ph.unito.it

Received 31 October 2000
Accepted 15 October 2001

regional climatology studies (Simmonds and Hope, 1997) seems to indicate a close correlation, particularly during some strong convective precipitation events, like the one that originated the flash flood of 12–14 September 1995 in South Ticino.

In the current paper, the 1995 South Ticino flash flood was analysed at a fine resolution with the help of a limited-area model (LAM), with particular emphasis to the soil moisture initialization, as a crucial component in the evaporation process over the land surface. The correct initialization of soil moisture can affect convective cell development and, therefore, be important for the short-term weather prediction. The sensitivity to initial soil moisture was tested on the intense precipitation event recorded on 1995 South Ticino flood.

The numerical model used for this simulation was the operational version of the LAM of Bologna (LAMBO), based on a 1989 version of the NCEP–ETA model, operational at the Regional Meteorological Service of the Emilia—Romagna Italian region. The initial data for LAMBO were the European Centre for Medium-Range Weather Forecasts (ECMWF) operational analyses. As initial soil moisture data, two different sources were compared: in one run, the ECMWF analyses were used; in the other, the results of the (climatology of parameters at the surface) (CLIPS) experiment (Cassardo *et al*., 1999a) were used. CLIPS was an experiment performed with the aim of creating a climatological archive of parameters such as soil and canopy temperature and moisture, turbulent and conductive heat fluxes, runoff and drainage, etc., not normally measured continuously at the mesoscale. The method consisted in the use of a soil–vegetation–atmosphere transfer (SVAT) scheme running on a point-based dataset composed of continuously (i.e. hourly) recorded observations. The area selected for this experiment was Northern Italy and the surroundings, and we used synoptic observations as input driving data. The model used was the Land Surface Process Model (LSPM), developed by Cassardo *et al*. (1995). In both cases, LAMBO was integrated for 24 h on a 15 km interval grid.

The problem of 'spin-up' for the soil conditions in LSPM was investigated by running the model for a time period of 5 months (from 1 May to 30 September 1995) and of 9 months (from 1 January to 30 September 1995), and verifying that the two runs produced the same results (Balsamo, 1999).

In this paper, the results of the two simulations carried out with the numerical model LAMBO are presented: the first simulation, based on the ECMWF data, will be called the 'control run', and the second simulation, using the CLIPS data, will be called the 'CLIPS run'.

THE METEOROLOGICAL SITUATION OF SOUTH TICINO 1995 CASE STUDY

On 13 September, the 500 hPa circulation became stronger and more meridional (Figure 1), and a cut-off minimum formed near Nice at 850 hPa (Figure 2), bringing warm and moist air from the Ligurian and Mediterranean Seas to the Alps. The frontal system was displaced in two parts due to the interaction with the Alps; the upper part was embedded in the cyclonic circulation and some active cumulonimbi were present in the western Alpine area. The effect of the warm air advection from the south was evident in the thermal vertical profile: the lower 6 km of troposphere were extremely moist and unstable. On 14 September the cyclone moved eastward and the post-frontal air, colder and less active than in the previous days, generated the scattered clouds present in the western Alps.

The maximum precipitation in the South Ticino area was observed in the period between 0600 GMT on 12 September and 0600 GMT on 13 September. Figure 3 shows the cumulated precipitation in the pluviometric high-resolution network of the Piedmont region (in this figure, a single pixel corresponds to 15×15 km^2). The most remarkable features were the peak over the South Ticino area (more than 200 mm of rainfall) and the wide area of precipitation greater than 100 mm over south-eastern France.

The situation selected was the remarkable flash flood that affected South Ticino (at the border between Switzerland and the Piedmont region, in north-western Italy) on 12–14 September 1995. This event was also selected as one of the case studies in the framework of the Mesoscale Alpine Programme (MAP), see Binder and Schär (1996).

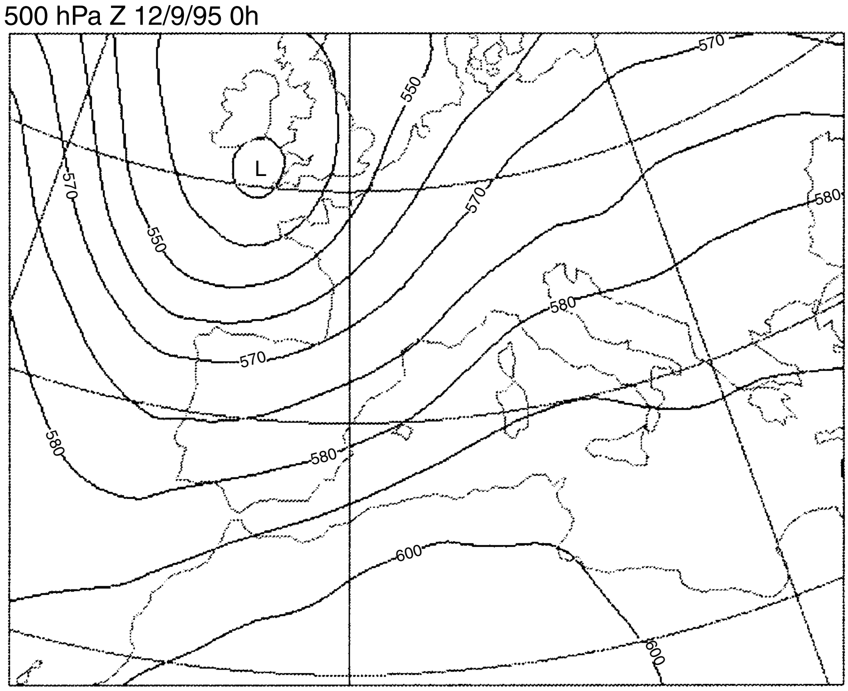

Figure 1. 500 hPa ECMWF analysis of 13 September 1995

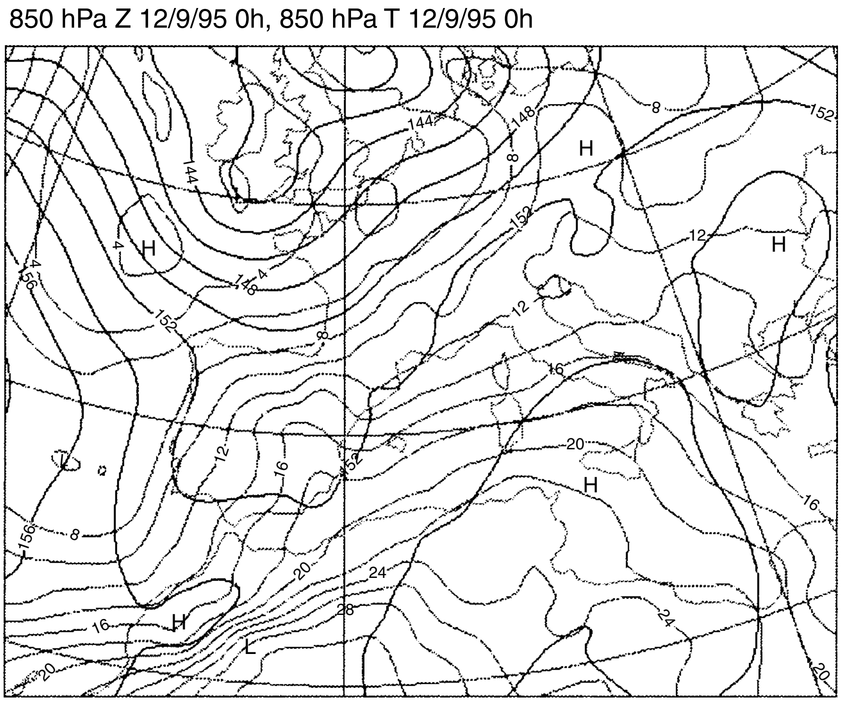

Figure 2. 850 hPa ECMWF analysis of 13 September 1995

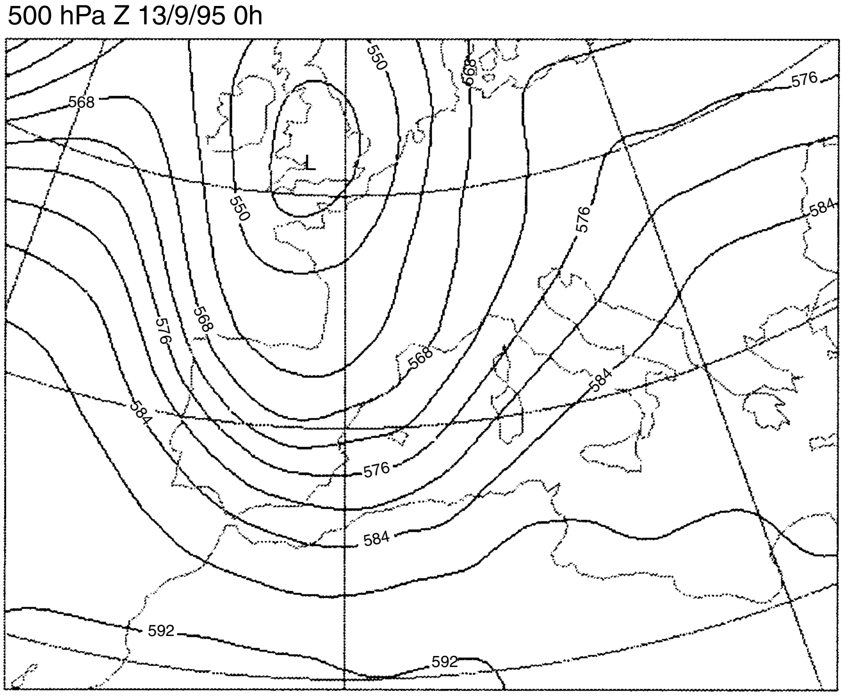

Figure 3. Precipitation cumulated in 24 h starting from 12 September 1995 at 0600 GMT detected by the pluviometric network of Piedmont Region

On 12 September, a frontal system was approaching the north-western side of the Alps; the cloudiness associated with this front in this northern part was essentially stratiform, while well-developed cumulonimbi were present in the southern part. This front was driven by a south-westerly circulation flow pattern (Figures 4 and 5 respectively show the 500 and 850 hPa ECMWF analyses for 12 September at 1200 GMT). The vertical thermal profile, in the zone of the approaching front, showed that the lower 4 km of the troposphere were moist and unstable.

THE MODELS

The LSPM (Cassardo *et al.*, 1995) was tested by Cassardo and coworkers (Ruti *et al.*, 1997; Cassardo *et al.*, 1998) and subsequently improved with the inclusion of a snow component (Loglisci *et al.*, 2001). LSPM is a typical SVAT scheme developed to be used both as a stand-alone model (in this case, a set of specific routines for the calculation of the input data was provided) and as the surface boundary subroutine of an atmospheric model (in this case, all input data were taken by the atmospheric model itself).

The schematic structure of the LSPM includes three main zones: the atmospheric layer above the vegetation extends between a reference height and the vegetation level (Figure 6). The hierarchy of the model allows a separation between the soil, canopy and atmospheric layers.

In the upper layer, all variables are calculated as weighted averages between bare soil and vegetated components. The canopy is considered as a uniform layer characterized by the following parameters: vegetation cover, height, leaf area index (LAI), albedo, minimum stomatal resistance, leaf dimension, emissivity, and root depth. Soil temperature and moisture are calculated using multi-layer schemes whose main parameters are: thermal conductivity, hydraulic conductivity, soil porosity, permanent wilting point, dry volumetric heat

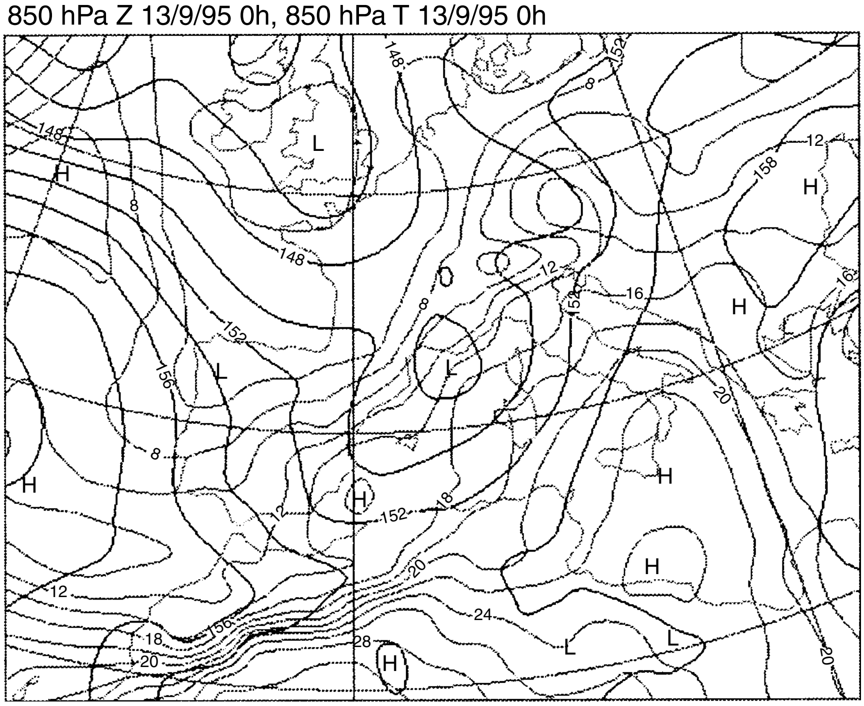

Figure 4. 500 hPa ECMWF analysis of 12 September 1995 at 1200 GMT

capacity, soil surface albedo and emissivity. The user can select a variable number of soil layers (fixed to nine in the present work). Each flux is partitioned according to the fractional covers of vegetation and snow. The model includes two subroutines for the long-wave and short-wave incoming radiation calculation, if these data are not observed (in this case, the cloud cover data are needed). The turbulent heat, water vapour and momentum fluxes are calculated by using the 'analogue electric' scheme, in which the flux is expressed as a ratio between a generalized gradient (of temperature or moisture) and resistances. The LSPM can provide the values of each component of soil thermal and hydrological budgets and of the water balance, and the turbulent fluxes.

The LAMBO is a version of the NCEP–ETA model with 32 vertical levels and a grid step of 15 km. The grid is rotated and staggered, corresponding to the class E grid according to Arakawa (1972). The radiative processes are implemented according to Geleyn and Hollingsworth (1979). For convection, the Betts and Miller (1986) parameterization is used and the Mellor and Yamada (1982) scheme for the surface layer is applied. The model uses a forward–backward finite difference method with an explicit time splitting (Mesinger and Arakawa, 1976). A nudging procedure was set in order to overcome the 'spin-up' and to adjust the initial conditions better to the observational data (Cacciamani *et al.*, 2000).

CLIPS EXPERIMENT: THE METHOD AND THE SET-UP OF THE DATA FOR LSPM

The initialization of soil properties (temperature, moisture content and land coverage) can strongly affect the quantitative precipitation forecast of a numerical model, especially when the moisture supply is provided by local evaporation. Nevertheless, routine observations of soil surface properties, like for instance soil moisture, are not generally available in real time on a wide area with a good horizontal resolution, except during

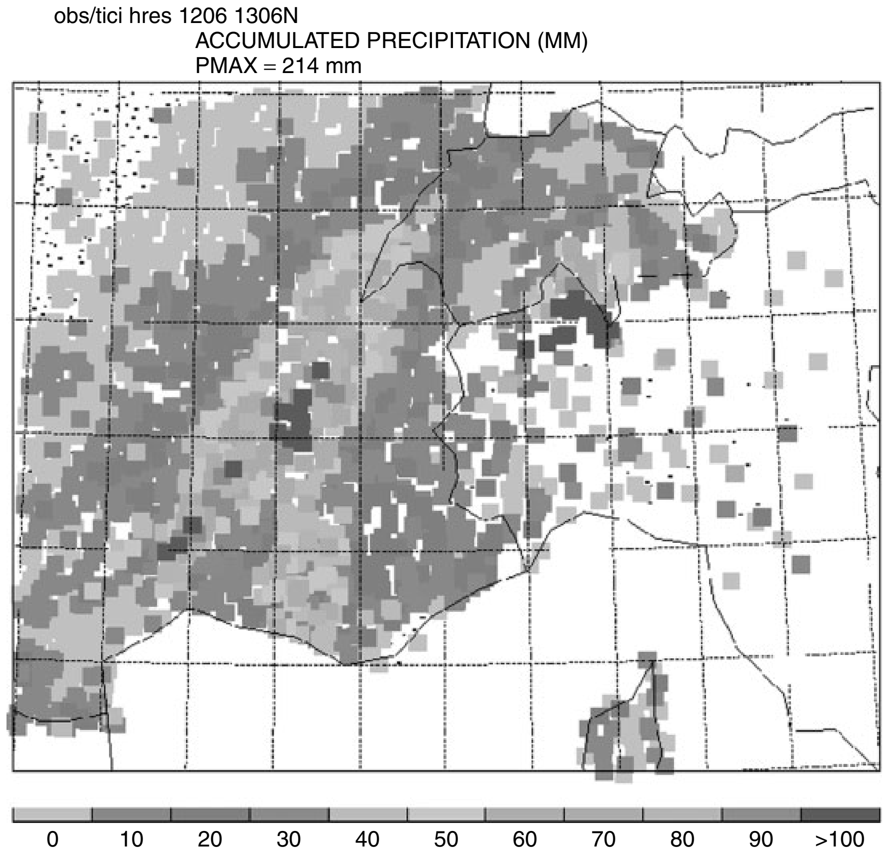

Figure 5. 850 hPa ECMWF analysis of 12 September 1995 at 1200 GMT

special field experiments whose temporal extension is normally limited to some days or weeks. For this reason, in this study it was decided to use the output of the LSPM–SVAT scheme, in order to calculate soil surface moisture fields at a given time. The data used to drive the simulation with LSPM in the 'stand-alone' version were gathered from synoptic observations of temperature, humidity, pressure, wind speed vector, precipitation and cloudiness. The surface fields obtained in this way can be used as initial conditions for LAM integration. This methodology was termed CLIPS (Cassardo *et al*., 1999a). Cassardo *et al*. (1999b) demonstrated that this method was able to provide realistic estimates of surface energy, thermal and hydrological budgets.

In this study, all synoptic observations in the rectangular area of longitude 4–20 °W and latitude 38–49 °N were considered. The semi-automatic stations were not included in the database, as generally they do not work for the whole day. Mountain stations (i.e. those altitude was higher than 1000 m) were not considered in this study because of the different elevations of the stations with respect to the LAMBO grid points, and also because the LSPM was not tested in mountainous areas. The total number of stations included in the database was 122. The area covered and the stations used are shown in Figure 7. For each synoptic station, temperature, relative humidity (or dew point temperature), wind velocities, total and low-cloud cover, precipitation and atmospheric pressure were selected. The period chosen for the simulations was 1 May–30 September 1995.

To remove gaps and inconsistencies from the dataset, the missing data were interpolated as the weighted averages of the nearest station measurements included in a radius of 300 km, using as weighting function the

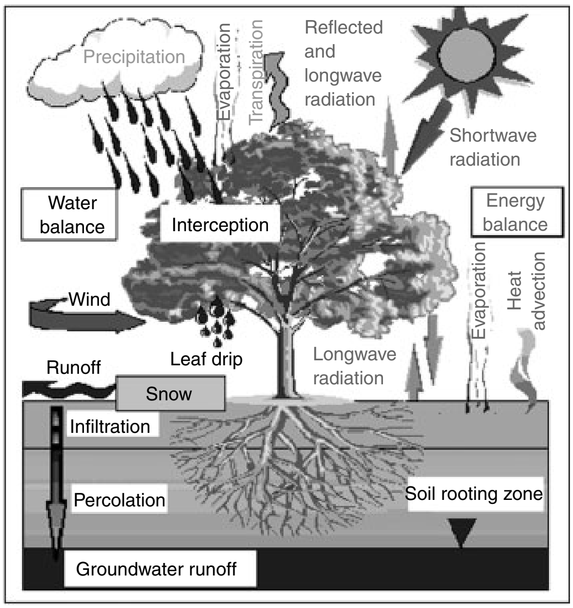

Figure 6. Schematic structure of the physical processes represented in the LSPM

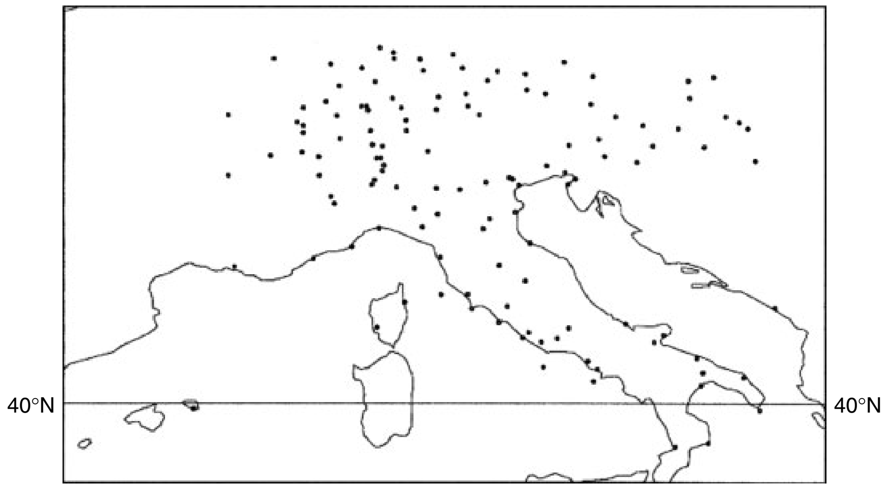

Figure 7. Map of the synoptic stations used in the frame of the CLIPS experiment

inverse of the square of distance:

$$\phi_i = \frac{\sum_{j=1}^{n} \frac{\phi_j}{r_j^2}}{R} \qquad \text{with} \qquad R = \sum_{j=1}^{n} \frac{1}{r_j^2} \tag{1}$$

where r_j is the distance between the station considered and the jth station; ϕ_i and ϕ_j are the observations of a generic variable carried out at the station considered and at the jth station respectively. Temperature and pressure data were scaled (to take into account the different elevation of the stations) using respectively the adiabatic lapse rate of the standard atmosphere and the hydrostatic equation. To increase the temporal resolution of the data (6 h for precipitation and 3 h for all other parameters) to the rate required by the LSPM (30 min), a mix of linear and cubic splines was applied to all data except precipitation (Ruti *et al*., 1997). The values of tension coefficient in the splines were selected according to the data's intrinsic variability (0·9 for the specific humidity and 0·1 for the others). Precipitation was assumed constant during the observing period. This rather crude assumption produced a redistribution of the observed peaks throughout the 6 h between two principal synoptic observations with a smoothing of the highest peaks, but it was the simplest method to conserve total precipitation.

A comparison of the data retrieved using the above interpolation techniques and the observations carried out at a higher acquisition rate (30 min) in a nearby station (San Pietro Capofiume, near Bologna, in the Po valley, Italy) was carried out over a period of 27 months (between January 1993 and March 1995). The results (Ruti *et al*., 1997; Balsamo, 1999) showed that the precipitation rate was consistently reduced by this method only in a few convective situations, mainly thunderstorms, whereas the specific humidity and the wind speed were in satisfactory agreement with the observations and all remaining data were in good agreement.

To confirm the validity of this method, the values observed in each station of the database were compared with the values interpolated in the locations of the station (Balsamo, 1999). The mean biases were lower for the stations surrounded by many other stations at a similar elevation, and generally ranged between 1 and 5%.

The soil type was assumed to belong to the class of loam for all stations, and the dominant vegetation type was short grass, according to specifications assumed for a typical synoptic site implantation. This assumption corresponded to the standard for synoptic stations according to the World Meteorological Organization requirements, and it was consistent with the soil type considered by the ECMWF model. The vegetation cover was assumed to vary between a winter minimum of 80% and a summer maximum of 95%. The root depth and the vegetation height were fixed at a value of 0·10 m.

The initial soil temperature and moisture for each station were calculated using the following formulations:

$$T(z) = \overline{T} + \Delta T \ \exp\left[\frac{-z}{D}\right] \ \sin\left[\frac{2\pi\left(M - 1 - \frac{1}{2}\right)}{12} - \frac{z}{D} - \frac{\pi}{2}\right]$$

$$Q_i(z) = F_c - F_c\left(1 - \frac{\overline{\mathrm{RH}}}{100}\right) \ \exp\left(-\frac{z}{D}\right) \qquad (2)$$

where z is the depth of the soil layer, D the soil depth at which the thermal amplitude is 1/e times its surface value ΔT, $\overline{T}$ is the mean temperature, M the month, F_c the field capacity and $\overline{\mathrm{RH}}$ the air mean relative humidity. ΔT was calculated as the difference between the monthly mean values of July and January, whereas $\overline{T}$ and $\overline{\mathrm{RH}}$ were calculated as the yearly mean values for any individual station. The first relationship is the analytical solution of the Fourier heat equation under the hypothesis of a sinusoidal forcing (Stull, 1988; Garratt, 1994). The second one has been originally developed in this work by analogy with the thermal equation for the temperature and considering that there is a relation between the atmospheric humidity and the soil moisture in regions characterized by low wind regimes, as in the Po valley in Italy.

The comparison between the values predicted by the previous expressions and the observations gathered at San Pietro Capofiume station (soil temperature at seven levels between soil surface and 1 m, soil moisture at 10 cm) during the 27 months of observations (January 1993–March 1995) showed that the thermal values were well captured by Equation (2) (Figure 8), and that the soil moisture values were mainly in agreement with the observations in winter time, whereas in summer there were some dry peaks not reproduced by Equation (2) (Figure 9).

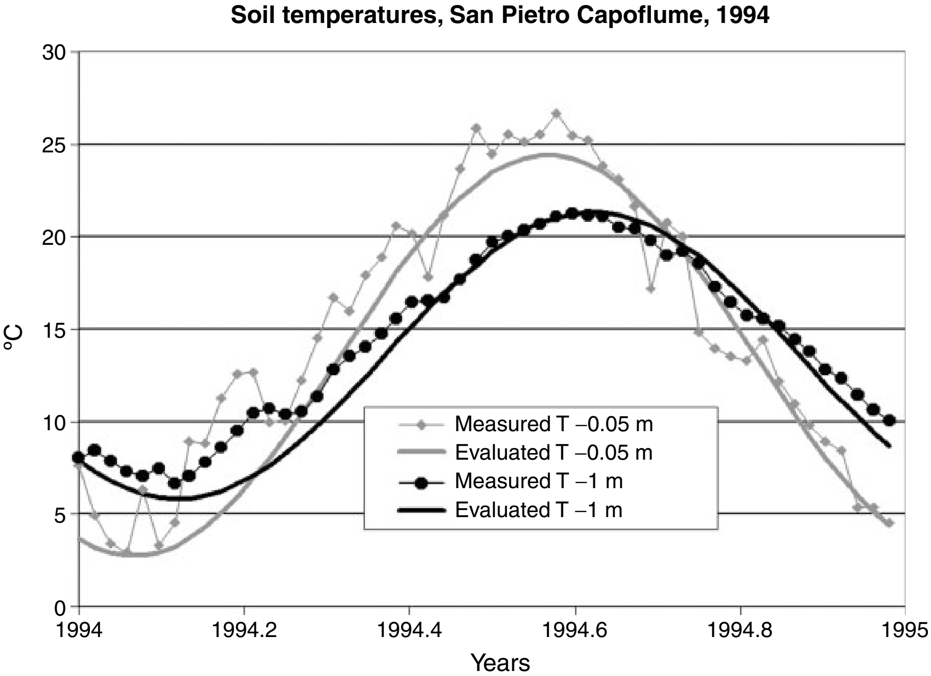

Figure 8. Comparison of the daily values of soil temperature at the two soil levels of 5 cm and 1 m; solid lines are the result of Equation (1) and points are the observations (weekly means) carried out at San Pietro Capofiume in 1993

RESULTS OF THE LSPM SIMULATIONS

The soil–vegetation system behaves like a water reservoir whose content varies in response to fluctuating supplies and demands, and a critical parameter that affects evaporation is the effective water-holding capacity of the soil (Milly and Dunne, 1994). For this reason, the time required to achieve the steady state in which the balance is not affected by the initial conditions can be considerably longer than the time scale used for weather forecasts. According to the results of previous tests (Cassardo *et al.*, 1997), in which it was verified that an integration period of about 6 months seemed to produce a final result independent from the initial conditions, it has been decided to run the LSPM for 5 months.

In order to verify that the results obtained did not depend on the initial values selected for soil properties, a longer run (9 months) was performed. By comparing the differences in the monthly mean values of September, we found a maximum difference of 0·1 °C for the soil and canopy temperatures (Figure 10) and 0·05% (expressed as a fraction of the soil porosity) for the soil moisture in all soil layers (Figure 11). Then, by running a long-lasting simulation with LSPM starting from 1 May and lasting until 30 September 1995, the following outputs were calculated: temperature and moisture in nine soil layers down to about 7 m, net radiation, turbulent (sensible and latent) and conductive (soil–atmosphere) heat fluxes, evaporation, runoff and drainage. The database of soil moisture was used as initial conditions for the LAMBO. The same procedure previously described in the CLIPS experiment was used to interpolate the synoptic stations spatially on the LAMBO regular grid, whose mesh size was $15 \times 15\ \mathrm{km}^2$.

Figure 12 shows the plots of initial soil moisture content (metres) in the first 10 cm of soil taken from the ECMWF (control plot) and calculated with the LSPM in the frame of the CLIPS experiment. As regards Figure 12b, it is necessary to underline that the soil moisture field was calculated over the

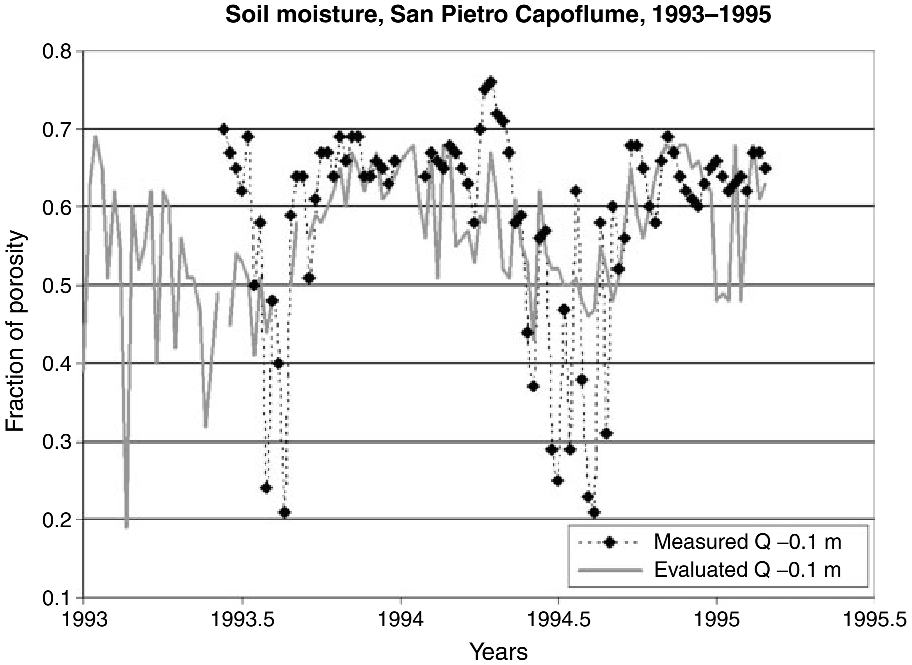

Figure 9. Same as Figure 8, but for soil moisture at 10 cm in 1993 and 1994. Soil moisture is expressed in fraction of porosity

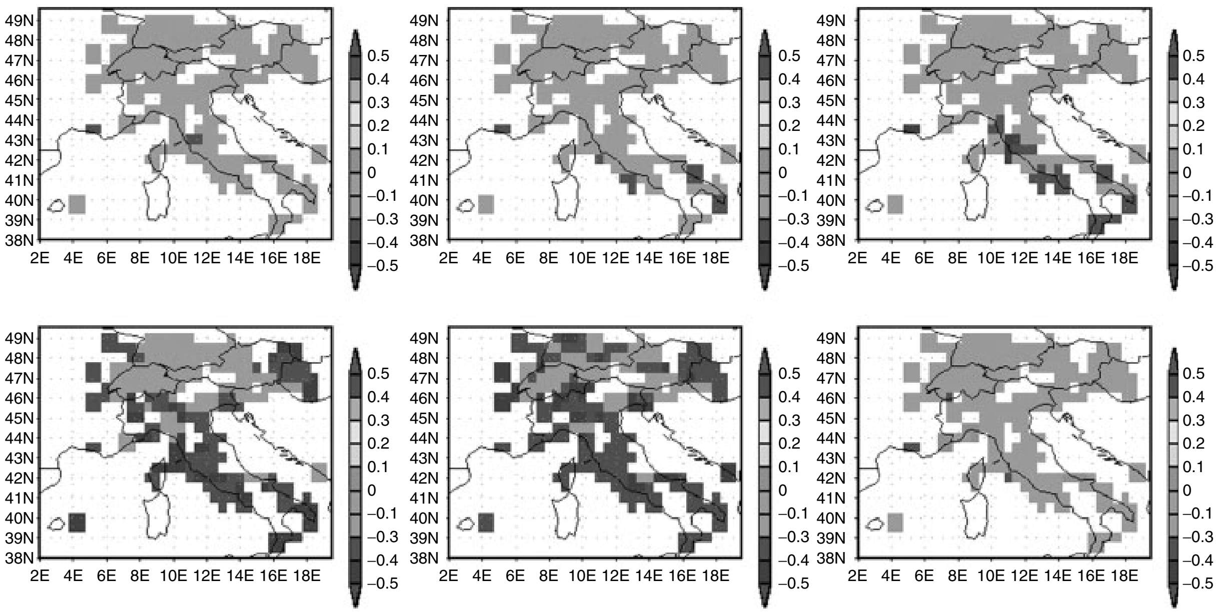

Figure 10. Differences between the September 1995 monthly mean temperatures in the soil and canopy calculated by the LSPM in the 9 month simulation and in the 5 month simulation: (a) soil temperature at 5 cm; (b) soil temperature at 20 cm; (c) soil temperature at 50 cm; (d) soil temperature at 1 m; (e) soil temperature at 2 m; (f) canopy temperature

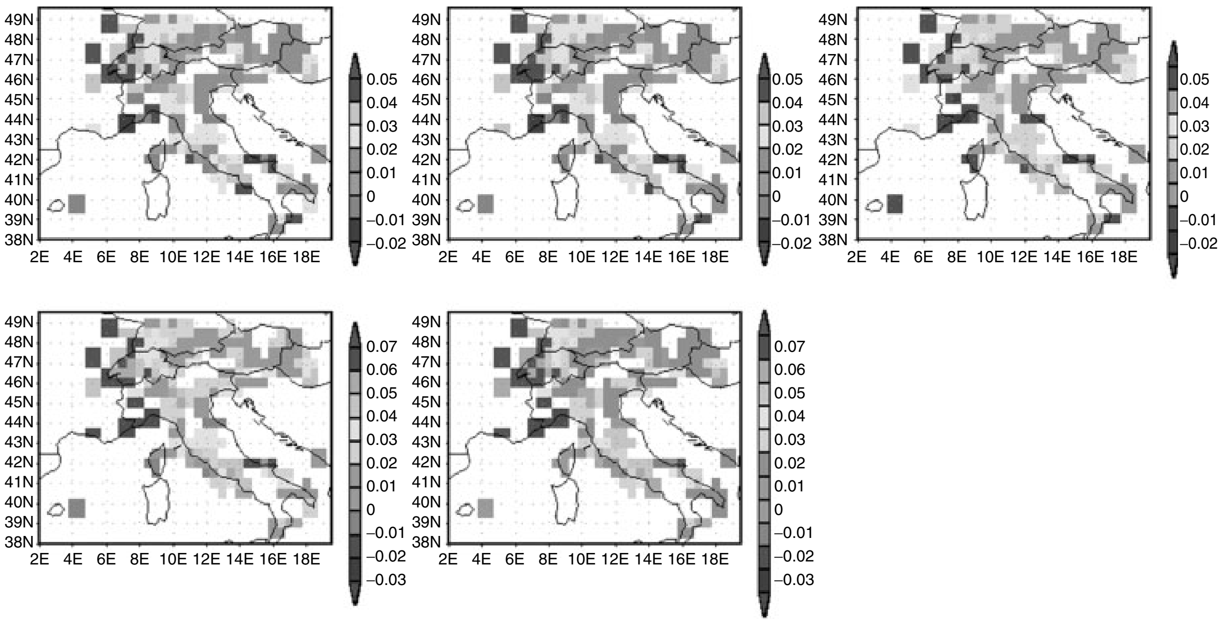

Figure 11. Differences between the September 1995 monthly mean soil moistures (expressed in units of the soil porosity) calculated by the LSPM in the 9 month simulation and in the 5 month simulation: (a) soil moisture at 5 cm; (b) soil moisture at 20 cm; (c) soil moisture at 50 cm; (d) soil moisture at 1 m; (e) soil moisture at 2 m

entire domain of the LAMBO, even if the coverage of the synoptic stations was not homogeneous throughout the area. For graphic reasons, this interpolated field is displayed in Figure 12b over the entire domain, but for the sake of comparison it is better to focus attention on the soil moisture values located inside the rectangular area of longitude 6–12 °E and latitude 43–48 °N. In this zone, the CLIPS soil moisture field appeared to be more structured, and the differences between the driest and the wettest regions were more evident that in the ECMWF field, which seemed practically constant throughout the whole domain, excepting for the relatively dry tongue on the western Alps. In particular, the numerical values of the soil moisture evaluated by the LSPM are lower than those coming from the ECMWF analyses.

RESULTS OF THE LAMBO SIMULATIONS

The influence of the different soil moisture initialization on the rainfall forecast is shown in Figure 13. The peak precipitation over South Ticino was still underestimated, but it increased from 91·5 to 110·0 mm, i.e. by about 20%. The wide area of precipitation over France (identified by the 40 mm contour in Figure 13) and the area without precipitation located on the Po valley were not affected by the change in the initial soil moisture content, meaning that the new soil moisture field did not produce spurious precipitation.

To obtain a more quantitative result, contingency tables (Wilks, 1995) covering the whole domain were analysed. Contingency tables allow a skill score to be assigned to the forecast. In fact, in the contingency table in Table I, the following quantities, defined as a function of the observed and predicted rainfall, are calculated: the percentage of successful predictions, i.e. the relative number of stations in which rainfall was correctly predicted and observed, and correctly not predicted and not observed (SUCC); the percentage of stations in which rainfall has been predicted and observed successfully (SUCCT); the percentage of stations in which rainfall has been not predicted and not observed (SUCCNT); the percentage of correct predictions

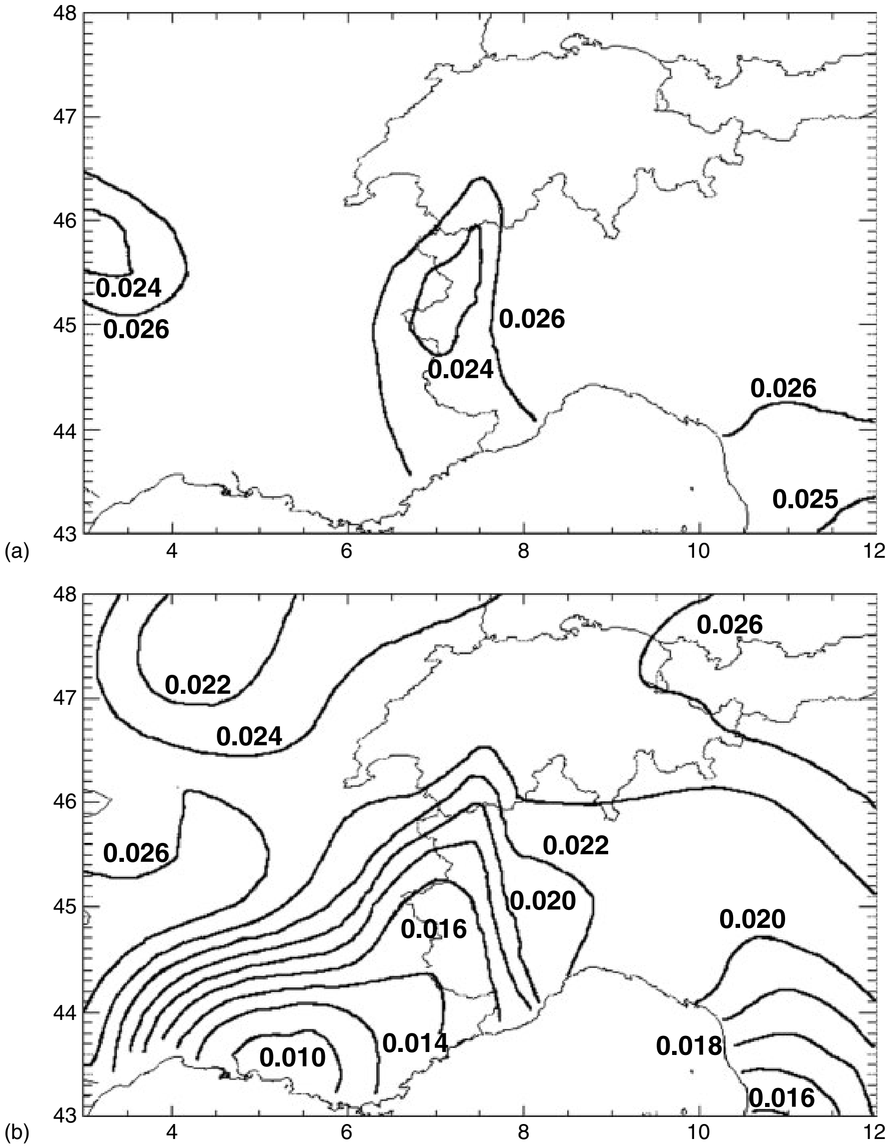

Figure 12. Initial field of soil moisture content (metres) on 12 September 1995 at 0600 GMT: (a) ECMWF; (b) LSPM

considering only rainfall episodes (THREAT); and the fractional bias (FBIAS), defined as the ratio between the number of stations in which precipitation has been predicted and the number of stations in which it has been observed. Clearly, the 'best' value for the first four indexes is 100 and for FBIAS it is unity. FBIAS represents the estimation tendency, and assumes values greater than unity in the case of overestimation and lower than unity in the case of underestimation.

The data used in this evaluation came from the high-resolution hydrologic network of the Piedmont Region, French and Swiss network, of which Figure 3, reporting the total precipitation cumulated during the flood episode, was a typical example. The LAMBO cumulated precipitation was interpolated at each individual station using the algorithm given by Equation (1). The values of the contingency table indexes were calculated

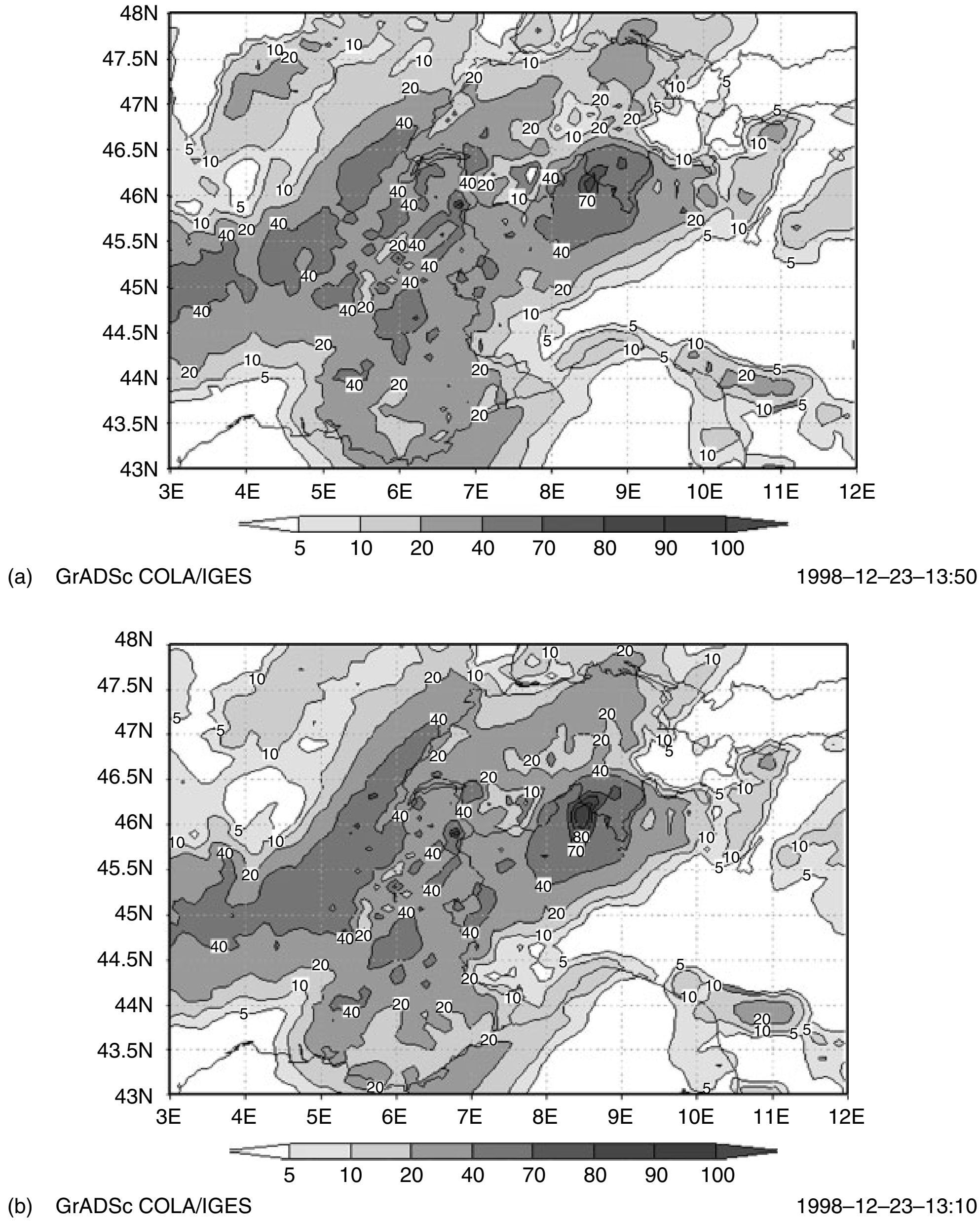

Figure 13. Cumulated precipitation on 24 h starting from 12 September 1995 at 0600 GMT: (a) control run; (b) CLIPS run

for precipitation thresholds of 0·5, 1, 2, 5, 10, 15, 20, 30, 40 and 50 mm for the control run (Table II) and the CLIPS run (Table III). Table IV reports the differences between Table II and III, and the values corresponding to an increase of the forecast skill are given in bold-face type.

This shows that forecasting skill was improved for all variables, except FBIAS, SUMB and SUMC. For SUMB and SUMC there was a decrease in the percentage (as the number of overestimations and underestimations decreased) and FBIAS became closer to unity. As expected, the improvements were small in absolute value for two reasons: because the grid area of the LAMBO mesh (225 km^2) was much larger

Table I. Equations used as the basis for the contingency table in Table II. For any given rainfall threshold, A is the number of correct rainfall predictions (rain predicted and observed), B the number of underestimated predictions (rain not predicted but observed), C the number of overestimated predictions (rain predicted but not observed) and D the number of correct 'non-rainfall' predictions (rain not predicted and not observed). Thus, SUCC is the percentage of successful predictions, SUCCT the percentage of successful predictions for rainfall episodes, SUCCNT the percentage of successful predictions for non-rainfall episodes, and THREAT the percentage of correct prediction considering only rainfall episodes. The fractional bias FBIAS is the estimation tendency

Variable	Expression	Best value
SUCC	$100\dfrac{A+D}{A+B+C+D}$	100
SUCCT	$100\dfrac{A}{A+B}$	100
SUCCNT	$100\dfrac{D}{C+D}$	100
THREAT	$100\dfrac{A}{A+B+C}$	100
FBIAS	$\dfrac{A+C}{A+B}$	1

Table II. Summary of statistical indexes obtained in the control run using ECMWF initialization

Rainfall threshold (mm)	SUCC	SUCCT	SUCCNT	THREAT	FBIAS	SUMA	SUMB	SUMC	SUMD
0·5	73·0	98·3	1·3	73·4	1·3	1505	26	520	7
1	69·0	97·2	2·5	69·0	1·4	1410	41	592	15
2	62·0	95·0	4·7	62·4	1·5	1262	66	696	34
5	54·0	90·8	10·9	52·2	1·6	1021	103	832	102
10	45·0	79·8	18·6	39·2	1·8	723	183	938	214
15	41·0	64·2	29·4	26·9	2·0	446	249	962	401
20	45·0	48·5	44·1	17·6	2·2	241	256	872	689
30	66·0	36·0	70·4	10·0	3·0	76	135	547	1300
40	94·0	31·0	96·4	13·7	1·6	18	40	73	1927
50	98·0	4·2	100·0	4·2	0·0	1	23	0	2034

than the size of the area affected by the heavy precipitation, and also because the contingency tables were calculated over the whole domain.

The improvements in SUCC and SUCCNT were caused by the improvement in the prediction of the precipitation thresholds between 2 and 30 mm (Table IV). There was also an increase in the accuracy of the rainfall prediction (SUCCT) for the thresholds greater than 10 mm, even if there was a slight increase in the underestimation for the 40 mm threshold (SUMC).

FBIAS for all the stations increased from a value of 0·52 in the control run to a value of 0·62 in the CLIPS run. The improvement of FBIAS was larger for the few stations in which the heaviest precipitation was observed (Table IV). All these values indicated that there was an improvement in rainfall prediction, even if the underestimation was still large. The improvements for all stations and all rainfall thresholds are shown in Table V.

Table III. Summary of statistical indexes obtained in the CLIPS run using LSPM initialization

Rainfall threshold (mm)	SUCC	SUCCT	SUCCNT	THREAT	FBIAS	SUMA	SUMB	SUMC	SUMD
0·5	73·0	98·1	1·7	73·3	1·3	1502	29	518	9
1	68·0	96·7	2·8	68·7	1·4	1403	48	590	17
2	63·0	95·1	5·9	62·7	1·5	1263	65	687	43
5	55·0	90·2	13·6	52·5	1·6	1014	110	807	127
10	49·0	82·7	23·4	41·9	1·8	749	157	883	269
15	46·0	71·5	33·5	31·0	2·0	497	198	907	456
20	51·0	60·0	48·5	22·9	2·2	298	199	804	757
30	67·0	40·3	70·7	11·3	3·0	85	126	542	1305
40	92·0	36·2	93·8	11·6	2·5	21	37	123	1877
50	98·0	12·5	99·8	10·7	0·3	3	21	4	2030

Table IV. Summary of the improvements obtained for each threshold obtained by the difference of the values reported in Tables II and III. The improved values in bold

Rainfall threshold (mm)	SUCC	SUCCT	SUCCNT	THREAT	FBIAS	SUMA	SUMB	SUMC	SUMD
0·5	0·0	−0·2	**0·4**	−0·1	0·0	−3·0	3·0	**−2.0**	2·0
1	−1·0	−0·5	**0·3**	−0·3	0·0	−7·0	7·0	**−2.0**	2·0
2	**1·0**	**0·1**	**1·2**	**0·3**	0·0	**1·0**	**−1.0**	**−9.0**	**9·0**
5	**1·0**	−0·6	**2·7**	**0·3**	0·0	−7·0	7·0	**−25·0**	**25·0**
10	**4·0**	**2·9**	**4·8**	**2·7**	0·0	26·0	**−26·0**	**−55·0**	55·0
15	**5·0**	**7·3**	**4·1**	**4·1**	0·0	51·0	**−51·0**	**−55·0**	**55·0**
20	**6·0**	**11·5**	**4·4**	**5·3**	0·0	57·0	**−57·0**	**−68·0**	**68·0**
30	**1·0**	**4·3**	**0·3**	**1·3**	0·0	9·0	**−9·0**	**−5·0**	**5·0**
40	−2·0	**5·2**	−2·6	−2·1	**0·9**	3·0	**−3·0**	50·0	−50·0
50	0·0	**8·3**	−0·2	**6·5**	**0·3**	2·0	**−2·0**	4·0	−4·0

Table V. Summary of the improvements obtained for all the thresholds (sum); all values represent an increase in forecast skill

SUCC	SUCCT	SUCCNT	THREAT	FBIAS	SUMA	SUMB	SUMC	SUMD
15	**38.3**	**15.4**	**18**	**1.2**	**132**	**−132**	**−167**	**167**

Interpreting these results is not easy and straightforward. In the CLIPS run, the soil moisture over the target area (South Ticino, but also the entire Alpine area) is approximately 6–10% lower than in the control run, and it is puzzling as to why a reduction in the soil moisture content, which is usually associated with a reduction in evaporation from the surface, leads to an increase in the precipitation maxima and alters the precipitation pattern. Looking at the upper air fields, both in their horizontal and vertical structure (maps not shown here), there are no clear indications about the possible mechanism causing the observed differences. No evidence of differences in the fields directly affecting the precipitation, like vertical stability or lower atmosphere moisture content, has been found, apart from very local and apparently negligible differences. The only impact of modified moisture analysis on the forecast is visible when looking at the lower troposphere horizontal wind field around the western Alpine region and the Mediterranean coast, where local reinforcement or weakening of mesoscale circulation can be detected. It is thus necessary to assume that, in this case, small differences are combined together by the complex feedback mechanisms of the atmosphere, producing as an overall effect the differences in the precipitation forecasts previously described.

CONCLUSIONS

The influence of the soil moisture initialization on the simulation of the flash flood episode that occurred during September 1995 in the South Ticino area of Switzerland was studied with the LAMBO, driven by ECMWF data.

The study was undertaken with two experiments. In the first one, the initial soil moisture provided by the ECMWF analyses was used. In the second one, the fields calculated in the frame of the CLIPS experiment were used as initial soil moisture. In this experiment, a SVAT scheme (LSPM) was driven by the synoptic observations carried out on a mesoscale area surrounding Northern Italy.

A check to see that the soil moisture field created in this way was not affected by the spin-up problem was done by comparing the results of two long runs of the LSPM, one of 5 months and the other of 9 months. The results were similar, meaning that the field had reached a stable state.

The results of the two simulations carried out with the LAMBO seemed to indicate that the precipitation field obtained for the flood episode in the second (CLIPS) experiment was closer to the observations than the one from the first experiment (ECMWF). In fact, even if there were still some disagreements between the observations and the LAMBO calculations (namely the LAMBO precipitation field was underestimated), the precipitation peak observed for South Ticino was closer to the observations, and the analysis of their distribution through the contingency tables showed an enhancement in the quality of the forecasts, even if the peak rainfall was still underestimated.

These results are encouraging because they seem to confirm that the initial soil moisture field can affect precipitation predictability in short-term weather forecasts. In particular, this case study showed that the mechanisms of interaction between soil moisture, surface evaporation and precipitation are complex, even if the conclusions from only one experiment must be regarded cautiously. In fact, the only impact of the modified moisture analysis field on the forecast is the variation of the mesoscale circulation around the western Alpine region and the Mediterranean coast. It is thus necessary to assume that, in this case, small differences are combined together by the complex feedback mechanisms of the atmosphere, producing as an overall effect the differences in the precipitation forecasts described in the paper.

The outcome of this work could be the realization of a coupled version of the LAMBO model and the LSPM in order to provide a better parameterization of the soil processes, as it could provide better short-term weather forecasts and improve the analysis of other similar events. A good database for further experiments would be the collection of cases within the framework of the MAP (Binder and Schär, 1996).

ACKNOWLEDGEMENTS

This work was done within the framework of the Mesoscale Alpine Programme and partially financed by the Italian CNR (National Council of Research) Project MAP, whose National Co-ordinator is Dr Andrea Buzzi, of CNR–ISAO in Bologna, Italy, and the local manager was Dr C. Cassardo. We were indebted to Mr A. Selvini and Dr M. Pantone of the Regional Meteorological Service of the Emilia–Romagna region for the help provided in the pre-processing and post-processing of the LAMBO simulations, and to Dr D. Gandini and Dr R. Cremonini of Piedmont Region for the help in the management of the station data.

REFERENCES

Arakawa A. 1972. *Design of the UCLA generation model. Numerical simulation of weather and climate*. Department of Meteorology, University of California, Los Angeles, Technical Report 7.

Balsamo GP. 1999. *Initialisation of land surface data in the atmospheric circulation models*. Unpublished thesis, Dipartimento di Fisica generale, Università, Via Pietro Giuria 1, 10125 Torino, Italy (in Italian).

Beljaars ACM, Viterbo P, Miller MJ, Betts AK. 1996. The anomalous rainfall over the United States during July 1993: sensitivity to land surface parameterization and soil moisture anomalies. *Monthly Weather Reviews* **124**: 362–383.

Betts AK, Ball JH. 1995. The FIFE surface diurnal cycle climate. *Journal Geophysical Research* **100**: 25 679–25 693.

Betts AK, Miller MJ. 1986. A new convective adjustment scheme: part II. *Quarterly Journal of the Royal Meteorological Society* **112**: 693–709.

Binder P, Schär C (eds). 1996. *MAP Design Proposal*. url:http://www.map.ethz.ch/.

Burde GI, Zangvil A, Lamb PJ. 1996. Estimating the role of local evaporation in precipitation for a two-dimensional region. *Journal of Climate* **9**: 1328–1338.

Cacciamani C, Cesari D, Grazzini F, Paccagnella T, Pantone M. 2000. Numerical simulation of intense precipitation events south of the Alps: sensitivity to initial conditions and horizontal resolution. *Meteorology and Atmospheric Physics* **72**(2–4): 31–42.

Cassardo C, Ji JJ, Longhetto A. 1995. A study of the performance of a land surface process model (LSPM). *Boundary Layer Meteorology* **72**: 87–121.

Cassardo C, Ruti PM, Cacciamani C, Longhetto A, Paccagnella T, Bargagli A. 1997. CLIPS experiment. First step: model intercomparison and validation against experimental data. *MAP Newsletter* **7**.

Cassardo C, Carena E, Longhetto A. 1998. Validation and sensitivity tests on improved parameterizations of a Land Surface Process Model (LSPM) in the Po Valley. *Il Nuovo Cimento* **21C**(2): 87–121.

Cassardo C, Balsamo GP, Pelosini R, Cacciamani C, Cesari D, Paccagnella T, Longhetto A. 1999a. Initialization of soil parameters in LAM: CLIPS experiment. *MAP Newsletter* **11**: 26–27.

Cassardo C, Balsamo GP, Pelosini R, Cacciamani C, Cesari D, Paccagnella T. 1999b. Effects of soil surface temperature and moisture initializations on the simulation of South Ticino 1995 flood with LAMBO. *MAP Newsletter* **11**: 28–29.

Eltahir EAB. 1998. A soil moisture rainfall feedback mechanism: 1. Theory and observations. *Water Resources Research* **34**: 765–776.

Findell KL, Eltahir EAB. 1997. An analysis of the relationships between spring soil moisture and summer rainfall, based on direct observations from Illinois. *Water Resources Research* **33**: 725–735.

Garratt JR. 1994. *The Atmospheric Boundary Layer*. Cambridge University Press: Cambridge.

Geleyn JF, Hollingsworth A. 1979. An economical analytical method for the computation of the interaction between scattered and line absorption of radiation. *Contributions for Atmospheric Physics* **52**: 1–16.

Loglisci N, Cassardo C, Balsamo GP, Qian MW. 2001. *A technical description of the Land Surface Process Model (LSPM), version 2000*. Internal Report DFG-8/2/2001, Dipartimento di Fisica Generale, Università di Torino, Via Pietro Giuria 1 10125 Torino, Italy.

Mahfouf J-F. 1991. Analysis of soil moisture from near-surface parameters: a feasibility study. *Journal of Applied Meteorology* **30**: 1534–1547.

Mellor GL, Yamada T. 1982. Development of a turbulence closure model for geophysical fluid problems. *Reviews in Geophysics and Space Physics* **20**: 851–875.

Mesinger F, Arakawa A. 1976. *Numerical Methods Used in Atmospheric Models*, vol. 1. GARP Publication Series, No. 17, WMO-ICSU Joint Organizing Committee, Geneva, 64 pp.

Milly PCD, Dunne KA. 1994. Sensitivity of the global water cycle to the water-holding capacity of land. *Journal of Climate* **7**: 506–514.

Rowntree PR, Bolton JA. 1983. Simulations of the atmospheric response to soil moisture anomalies over Europe. *Quarterly Journal of the Royal Meteorological Society* **109**: 501–526.

Ruti PM, Cassardo C, Cacciamani C, Paccagnella T, Longhetto A, Bargagli A. 1997. Intercomparison between BATS and LSPM surface schemes, using point micrometeorological data set. *Beitrage zur Physik der Atmospheric* **70**(3): 210–220.

Schär C, Frei C, Lüthi D, Davies HC. 1996. Surrogate climate change scenarios for regional climate models. *Geophysical Research Letters* **23**: 669–672.

Shukla J, Mintz Y. 1982. Influence of land-surface evapotranspiration on the Earth's climate. *Science* **215**: 1498–1501.

Simmonds I, Hope P. 1997. Persistence characteristics of Australian rainfall anomalies. *International Journal of Climatology* **17**: 597–613.

Stull RB. 1988. *An Introduction to Boundary Layer Meteorology*. Kluwer Academic Publishers: Dordrecht.

Viterbo P. 1995. Initial values of soil water and the quality of the summer forecasts. *ECMWF Newsletter* **69**: 2–8.

Wilks DS. 1995. *Statistical Methods in the Atmospheric Sciences: an Introduction*. Academic Press: London; 465 pp.

Zeng W, Dickinson RE, Zeng X. 1996. Climatic impact of Amazon deforestation: a mechanistic model study. *Journal of Climate* **9**(4): 859–883.

